

## Synthesis, structure, photophysical and electrochemiluminescence properties of Re(I) tricarbonyl complexes incorporating pyrazolyl–pyridyl-based ligands†

Qiao-Hua Wei,<sup>\*a,b</sup> Fang-Nan Xiao,<sup>a</sup> Li-Jing Han,<sup>a</sup> Shen-Liang Zeng,<sup>a</sup> Ya-Nan Duan<sup>a</sup> and Guo-Nan Chen<sup>\*a</sup>

Received 5th January 2011, Accepted 2nd March 2011

DOI: 10.1039/c1dt00015b

Three rhenium carbonyl complexes **1–3** were synthesized by reaction of the appropriate bidentate pyrazolyl–pyridyl-based ligand L1, L2 (L1 = 2-[1-{4-(bromomethyl)benzyl}-1*H*-pyrazol-3-yl]pyridine; L2 = 1,4-bis(3-(2-pyridyl)pyrazol-1-ylmethyl)benzene) with [Re(CO)<sub>3</sub>Cl] in toluene. They were characterized by elemental analyses, ESI–MS, <sup>1</sup>H spectroscopy, and X-ray crystallography for **1** and **2**. Compounds **1–3** exhibit bright yellow–green luminescence in the solid state and in solution at 298 K with the lifetimes in the microsecond range. It is noteworthy that the luminescent quantum efficiencies of compounds **1–3** are between 0.040 and 0.051, which are much higher than that of the [Re(bpy)(CO)<sub>3</sub>Cl] complex (= 0.019) (M. M. Richter *et al.*, *Anal. Chem.*, 1996, **68**, 4370; J. Van Houten *et al.*, *J. Am. Chem. Soc.*, 1976, **98**, 4853). Electrogenerated chemiluminescence (ECL) was observed in solutions of these complexes in the absence or presence of coreactant tri-*n*-propylamine (TPrA) or 2-(dibutylamino)ethanol (DBAE) by stepping the potential of a Pt disk working electrode. The ECL spectra are identical to the photoluminescence spectra, indicating that the chemical reactions following electrochemical oxidation or reduction form the same <sup>3</sup>MLCT excited states as that generated in the photoluminescence experiments. In most cases, the ECL quantum efficiencies of complexes **1–3** are comparable to that of the [Re(L)(CO)<sub>3</sub>Cl] (L = bpy or phen) system. Oxygen tends to substantially decrease ECL intensities of the three rhenium complexes–TPrA system, which could allow them to be used as oxygen sensors.

## Introduction

Electrogenerated chemiluminescence (ECL) is the process of generating excited states in a photoactive molecule at an electrode surface, leading to luminescence upon return to the ground state. The design and synthesis of molecules that have reliable ECL properties have been attracted considerable interest,<sup>1–5</sup> since Hercules and Bard *et al.* reported the first ECL system in the mid-1960s.<sup>6</sup> In the past several years, a number of new ECL-emitting species, especially organometallic complexes, have been

synthesized and their ECL properties have been investigated.<sup>2,3,7–9</sup> At present, the mostly thoroughly studied on organometallic complexes as ECL candidates are [Ru(bpy)<sub>3</sub>]<sup>2+</sup> (bpy = 2,2'-bipyridine) and its derivatives because of their excellent photochemical and electrochemical properties. Such complexes are widely used in analytical applications, especially in clinical diagnostics and bimolecular detection.<sup>10–16</sup> Compared to other d<sup>6</sup> transition metals Ru(II) and Os(II)<sup>17</sup> tris-diimine systems, the ECL properties of rhenium tricarbonyl containing bidentate polypyridyl ligands have been less studied, although many exhibit strong photoluminescence in solution. To the best of our knowledge, the only reported ECL of a rhenium complex is [Re(L)(CO)<sub>3</sub>Cl] (where L is bpy, 1,10-phenanthroline (phen), or a methyl-substituted derivative).<sup>18,19</sup>

Since the ECL emission spectrum of [Re(L)(CO)<sub>3</sub>Cl] is similar to that of the optical emission spectrum and is assigned to emission from the lowest energy, <sup>3</sup>MLCT state,<sup>18</sup> subtle ligand modification can be sufficient to cause a significant change of the ECL properties. We and other groups have described recently a series of metal complexes which are bridged by a bidentate pyrazolyl–pyridine ligand.<sup>20–22</sup> The π\* orbital (LUMO) energy of the pyrazolyl–pyridine ligand is higher than that of the bpy ligand, which may result in a negative shift of the reduction

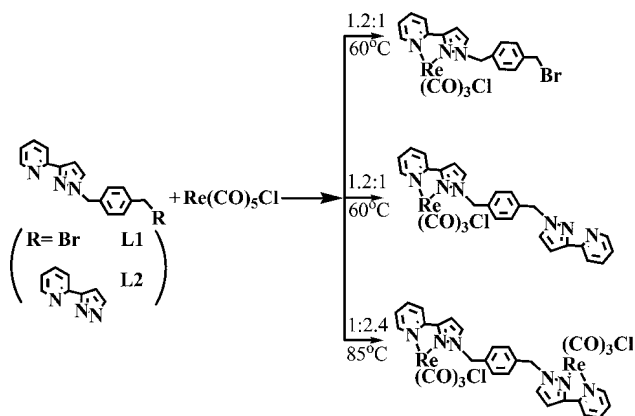
<sup>a</sup>Ministry of Education Key Lab of Analysis and Detection for Food Safety, Fujian Provincial Key Lab of Analysis and Detection for Food Safety, and Department of Chemistry, Fuzhou University, Fuzhou, 3500108, China. E-mail: qhw76@fzu.edu.cn, gnchen@fzu.edu.cn; Fax: 86 59122866135

<sup>b</sup>State Key Laboratory of Structural Chemistry, Fujian Institute of Research on the Structure of Matter and Graduate School of CAS, The Chinese Academy of Sciences, Fuzhou, Fujian, 350002, China

† Electronic supplementary information (ESI) available: X-ray crystallographic files in CIF format for the structure determination of compounds **1** and **2**; unit cell pack structure of complex **1** and **2**; CVs of 1 mmol L<sup>-1</sup> **1** in acetonitrile solution at different scan rates and relationship curves of the peak currents and scan rate; CVs of 1 mmol L<sup>-1</sup> L1 and L2 in acetonitrile solution at a scan rate of 100 mV s<sup>-1</sup>. CCDC reference numbers 806767 and 806768. For ESI and crystallographic data in CIF or other electronic format see DOI: 10.1039/c1dt00015b

potential of its metal complexes. These considerations prompted us to synthesize the rhenium tricarbonyl complexes containing bidentate pyrazolyl–pyridine ligand and investigate where they can be used for the production of ECL.

In this paper, three rhenium carbonyl complexes incorporating bidentate pyrazolyl–pyridyl-based ligands (as shown in Scheme 1) were synthesized and characterized. Their photophysical properties, electrochemical and ECL characteristics in the absence or presence of coreactant tri-*n*-propylamine (TPrA) or 2-(dibutylamino)ethanol (DBAE) were also extensively evaluated.



Scheme 1 Synthesis of compounds 1–3.

## Experimental

### Materials

All synthetic operations were performed under dry nitrogen atmosphere using Schlenk techniques and vacuum-line systems.  $[\text{Re}(\text{CO})_5\text{Cl}]$  and tetrabutylammonium hexafluorophosphate ( $\text{Bu}_4\text{NPF}_6$ ) were purchased from Alfa Aesar. All reagents were used as received and solvents were purified by standard methods. 3-(2-pyridyl)pyrazole,<sup>23</sup> 2-[1-{4-(bromomethyl)benzyl}-1*H*-pyrazol-3-yl]pyridine (L1) and 1,4-bis(3-(2-pyridyl)pyrazol-1-ylmethyl)benzene (L2) were prepared according to the published methods.<sup>24</sup>

### Synthesis

**$[\text{Re}(\text{L1})(\text{CO})_3\text{Cl}]$  (1).** The ligand L1 (196.9 mg, 0.60 mmol) and  $[\text{Re}(\text{CO})_5\text{Cl}]$  (180.8 mg, 0.50 mmol) in toluene were heated to 60 °C with vigorous stirring for 5 h. The solvent was removed under vacuum and the yellow residue was dissolved with 5 mL of dichloromethane and 30 mL of diethyl ether. The yellow solution was cooled in the refrigerator for several hours to give yellow prism crystals. Yield: 60%. Anal. calcd for  $\text{C}_{19}\text{H}_{14}\text{N}_3\text{O}_3\text{ReBrCl}$ : C, 36.02; H, 2.23; N, 6.64, found: C, 36.15; H, 2.23; N, 6.33. ESI–MS [ $m/z$  (%): 634 (30) [M], 248 (100) [M –  $\text{Re}(\text{CO})_3\text{Cl}$ ]. IR (KBr,  $\nu_{\text{cm}^{-1}}$ ): 2025 (s, CO), 1910 (s, CO), 1893 (s, CO).  $^1\text{H}$  NMR ( $\text{CDCl}_3$ , ppm): 8.90 (1H, d,  $J = 5.0$  Hz; pyridyl  $\text{H}^6$ ), 8.11 (1H, m, pyridyl  $\text{H}^3$ ), 7.93 (1H, d,  $J = 2.75$  Hz; pyridyl  $\text{H}^4$ ), 7.52–7.41 (2H, m, 2 × phenyl), 7.26–7.16 (4H, m; 2 × phenyl, pyrazolyl  $\text{H}^5$ , and pyridyl  $\text{H}^5$ ), 6.92 (1H, d,  $J = 2.75$  Hz; pyrazolyl  $\text{H}^4$ ), 5.69 (2H, d,  $J = 13.0$  Hz;  $\text{CH}_2$ -pz), 4.60 (2H, d,  $J = 19.50$  Hz;  $\text{CH}_2\text{Br}$ ).

**$[\text{Re}(\text{L2})(\text{CO})_3\text{Cl}]$  (2).** A mixture of L2 (239.2 mg, 0.61 mmol),  $[\text{Re}(\text{CO})_5\text{Cl}]$  (180.8 mg, 0.50 mmol), toluene (5 mL) was heated

to 60 °C with vigorous stirring for 12 h. The red solution was distilled off under vacuum, and the residue was dissolved in 2 mL dichloromethane. Diffusion of diethyl ether vapor onto the dichloromethane solution gave yellow crystals of **2**. Yield: 76%.  $\text{C}_{27}\text{H}_{20}\text{ClN}_6\text{O}_3\text{Re}$ : C, 46.41; H, 2.89; N, 12.04. Found: C, 46.13; H, 2.91; N, 12.34. ESI–MS [ $m/z$  (%): 699.5 (100) [M+H]<sup>+</sup>. IR (KBr,  $\nu_{\text{cm}^{-1}}$ ): 2019 (s, CO), 1920 (s, CO), 1887 (s, CO).  $^1\text{H}$  NMR ( $\text{CDCl}_3$ , ppm): 8.95 (1H, d,  $J = 4.0$  Hz; coordinated pyridyl  $\text{H}^6$ ), 8.63 (1H, d,  $J = 4.0$  Hz; pendant pyridyl  $\text{H}^6$ ), 7.96 (1H, ddd,  $J = 1.2, 1.6, 8.0$  Hz; coordinated pyridyl  $\text{H}^3$ ), 7.92 (1H, d,  $J = 1.2$  Hz; coordinated pyridyl  $\text{H}^4$ ), 7.86 (1H, d,  $J = 0.8$  Hz; pendant pyridyl  $\text{H}^4$ ), 7.71 (1H, ddd,  $J = 1.2, 1.6, 8.0$  Hz; pendant pyridyl  $\text{H}^3$ ), 7.47 (1H, d,  $J = 2.4$  Hz; coordinated pyrazolyl  $\text{H}^5$ ), 7.42–7.40 (2H, m, 2 × phenyl), 7.30–7.18 (5H, m; 2 × phenyl, coordinated pyrazolyl  $\text{H}^4$ , and 2 × pyridyl  $\text{H}^5$ ), 6.92 (1H, d,  $J = 2.4$  Hz; pendant pyrazolyl  $\text{H}^5$ ), 6.87 (1H, d,  $J = 2.8$  Hz; pendant pyrazolyl  $\text{H}^4$ ), 5.63 (2H, s,  $\text{CH}_2$ -coordinated pyrazolyl), 5.41 (2H, s,  $\text{CH}_2$ -pendant pyrazolyl).

**$[\text{Re}(\text{CO})_3\text{Cl}]_2\text{L2}$  (3).** L2 (115.2 mg, 0.29 mmol) and  $[\text{Re}(\text{CO})_5\text{Cl}]$  (236.1 mg, 0.65 mmol) in toluene (5 mL) were heated to 85 °C with stirring for 12 h. The crude product was collected by filtration and recrystallized from DMF–diethyl ether to give **3** as yellow powders. Yields: 92%. Anal. calcd for  $\text{C}_{30}\text{H}_{20}\text{Cl}_2\text{N}_6\text{O}_6\text{Re}_2$ : C, 35.89; H, 2.01; N, 8.37. Found: C, 35.81; H, 1.91; N, 7.89. ESI–MS,  $m/z$ : 1039.9 (100) [M + Cl]<sup>+</sup>. IR (KBr,  $\nu_{\text{cm}^{-1}}$ ): 2024 (s, CO), 1909 (s, CO), 1886 (s, CO).  $^1\text{H}$  NMR ( $\text{D}_3\text{CON}(\text{CD}_3)_2$ , ppm): 8.90 (2H, d,  $J = 5.2$ , pyridyl  $\text{H}^6$ ), 8.37 (2H, d,  $J = 4.0$ , pyridyl  $\text{H}^3$ ), 8.32 (2H, t,  $J = 5.2$ , pyridyl  $\text{H}^4$ ), 8.27 (2H, td,  $J = 6.8, 1.2$  Hz, pyrazolyl  $\text{H}^5$ ), 7.62 (2H, ddd,  $J = 6.4, 2.8, 1.6$ , pyridyl  $\text{H}^5$ ), 7.46 (2H, t,  $J = 2.8$  Hz, pyrazolyl  $\text{H}^4$ ), 7.24 (4H, s, phenyl), 5.83 (2H, d,  $J = 16$  Hz,  $\text{CH}_2$ ), 5.58 (2H, d,  $J = 16.4$  Hz,  $\text{CH}_2$ ).

### Crystal structural determination

Crystal **1** coated with epoxy resin was measured on a BRUKER SMART CCD diffractometer by  $\omega$  scan technique at 150 K with graphite-monochromated Mo-K $\alpha$  ( $\lambda = 0.71073$  Å) radiation, and crystal **2** was measured on a BRUKER P4 diffractometer by  $\omega$  scan technique at 293 K at Fujian Institute of Research on the Structure of Matter, the Chinese Academy of Sciences. An absorption correction by SADABS was applied to the intensity data. The structures were solved by direct methods or by the Patterson procedure and the heavy atoms were located from an *E*-map. The remaining non-hydrogen atoms were determined from the successive difference Fourier syntheses. All non-hydrogen atoms were refined anisotropically except those mentioned otherwise. The hydrogen atoms were generated geometrically with isotropic thermal parameters. The structures were refined on  $F^2$  by full-matrix least-squares methods using the SHELXTL-97 program package.<sup>25</sup> Crystallographic data of **1** and **2** are summarized in Table 1. Full crystallographic data are provided in the CIF files (ESI<sup>†</sup>).

### Physical measurements

Elemental analyses (C, H, N) were carried out on a Perkin–Elmer model 240 C automatic instrument. Electrospray mass spectra (ESI–MS) were recorded on a Finnigan LCQ mass spectrometer using dichloromethane–methanol or acetonitrile–methanol as the mobile phase. UV–Vis absorption spectra in acetonitrile, DMF

**Table 1** Crystallographic data for compounds **1**-DMF and **2**

Compound	<b>1</b> -DMF	<b>2</b>
Empirical formula	C <sub>41</sub> H <sub>35</sub> Br <sub>2</sub> Cl <sub>2</sub> N <sub>7</sub> O <sub>7</sub> Re <sub>2</sub>	C <sub>27</sub> H <sub>20</sub> ClN <sub>6</sub> O <sub>3</sub> Re
Formula weight	1340.88	698.14
Space group	<i>P</i> $\bar{1}$	<i>P</i> $\bar{1}$
<i>a</i> /Å	13.2187 (6)	10.360 (2)
<i>b</i> /Å	13.2825 (5)	10.530 (2)
<i>c</i> /Å	14.5639 (6)	12.400 (3)
$\alpha$ /deg	96.440 (2)	72.32 (3)
$\beta$ /deg	114.512 (2)	85.05 (3)
$\gamma$ /deg	105.043 (2)	69.03 (3)
<i>V</i> /Å <sup>3</sup>	2175.44 (16)	1203.1 (4)
<i>Z</i>	2	2
$\rho_{\text{calc}}$ /g cm <sup>-3</sup>	2.047	1.927
$\mu$ /mm <sup>-1</sup>	7.577	5.206
radiation ( $\lambda$ , Å)	0.71073	0.71073
Temp/K	150 (2)	293 (2)
<i>R</i> 1 ( <i>F</i> <sub>o</sub> ) <sup>a</sup>	0.0513	0.0294
<i>wR</i> 2( <i>F</i> <sub>o</sub> ) <sup>b</sup>	0.1433	0.0641
GOF	1.034	1.120

$$^a R1 = \sum |F_o - F_c| / \sum F_o \quad ^b wR2 = \sum [w(F_o^2 - F_c^2)] / \sum [w(F_o^2)]^{1/2}$$

and dichloromethane solutions were measured on a Perkin–Elmer Lambda 25 UV-Vis spectrometer. Infrared spectra were recorded on a Magna750 FT-IR spectrophotometer with KBr pellet. <sup>1</sup>H NMR spectra were measured on a BRUKER AVANCE III 400 MHz spectrometer with SiMe<sub>4</sub> as the internal reference. Emission and excitation spectra were recorded on a Perkin–Elmer LS 55 luminescence spectrometer with a red-sensitive photomultiplier type R928. Emission lifetimes were determined on an Edinburgh Analytical Instrument (F900 fluorescence spectrometer) using LED laser at 340 nm excitation and the resulting emission was detected by a thermoelectrically-cooled Hamamatsu R3809 photomultiplier tube. The instrument response function at the excitation wavelength was deconvoluted from the luminescence decay. The electrochemical and electrochemiluminescent (ECL) measurements were performed at room temperature using a system made in our lab,<sup>26</sup> consisting of a BPCL Ultra-Weak Chemiluminescence analyzer controlled by a personal computer (Institute of Biophysics, Chinese Academy of Sciences) in conjunction with a CHI model 1210 electrochemical analyzer (Shanghai Chenghua Instrument Co., China). A three-electrode system was employed with platinum wire as auxiliary electrode, SCE as reference electrode, and platinum disk electrode (2 mm diameter) as working electrode.

## Results and discussion

### Synthesis and characterization

The mononuclear complexes **1–2** (Scheme 1) were prepared in good yields by reaction of the appropriate pyrazolyl–pyridyl-based ligand (L1, L2) with [Re(CO)<sub>5</sub>Cl] (in 1.2 : 1 molar ratio) in toluene solution at 60 °C under N<sub>2</sub>, and recrystallized from CH<sub>2</sub>Cl<sub>2</sub>–diethyl ether, while the complex **3** was synthesized by reaction of L2 ligand with [Re(CO)<sub>5</sub>Cl] in 1 : 2.4 molar ratio in toluene solution at 85 °C, and recrystallized from DMF–diethyl ether. The reaction to prepare complex **2** in toluene solution requires a small excess of the L2 ligand and requires the careful control of the temperature to prevent further reaction to dinuclear complex **3**. Compounds

**Table 2** Selected bond distances (Å) and angles (°) for complex **1**

Re(1)–C(3)	1.904(9)	Re(2)–C(32)	1.904(11)
Re(1)–C(2)	1.918(9)	Re(2)–C(33)	1.914(9)
Re(1)–C(1)	1.925(9)	Re(2)–C(31)	1.917(10)
Re(1)–N(2)	2.161(7)	Re(2)–N(5)	2.163(8)
Re(1)–N(1)	2.201(7)	Re(2)–N(4)	2.191(8)
Re(1)–Cl(1)	2.5428(16)	Re(2)–Cl(2)	2.5313(16)
O(1)–C(1)	1.144(11)	O(4)–C(31)	1.145(12)
O(2)–C(2)	1.156(11)	O(5)–C(32)	1.162(12)
O(3)–C(3)	1.156(11)	O(6)–C(33)	1.158(11)
C(3)–Re(1)–C(2)	88.9(4)	C(32)–Re(2)–C(31)	89.8(4)
C(3)–Re(1)–C(1)	90.6(4)	C(32)–Re(2)–C(33)	90.4(4)
C(2)–Re(1)–C(1)	89.7(4)	C(33)–Re(2)–C(31)	90.0(4)
C(3)–Re(1)–N(2)	93.9(3)	C(33)–Re(2)–N(5)	94.2(3)
C(2)–Re(1)–N(2)	101.3(3)	C(32)–Re(2)–N(5)	100.3(3)
C(1)–Re(1)–N(2)	168.2(3)	C(31)–Re(2)–N(5)	168.9(4)
C(3)–Re(1)–N(1)	95.9(3)	C(33)–Re(2)–N(4)	97.1(3)
C(2)–Re(1)–N(1)	173.4(3)	C(32)–Re(2)–N(4)	170.7(4)
C(1)–Re(1)–N(1)	94.8(3)	C(31)–Re(2)–N(4)	95.7(4)
N(2)–Re(1)–N(1)	73.9(3)	N(5)–Re(2)–N(4)	73.6(3)
C(3)–Re(1)–Cl(1)	178.9(3)	C(33)–Re(2)–Cl(2)	179.1(3)
C(2)–Re(1)–Cl(1)	91.4(2)	C(32)–Re(2)–Cl(2)	89.7(3)
C(1)–Re(1)–Cl(1)	90.4(3)	C(31)–Re(2)–Cl(2)	91.0(3)
N(2)–Re(1)–Cl(1)	84.98(19)	N(5)–Re(2)–Cl(2)	84.86(19)
N(1)–Re(1)–Cl(1)	83.70(18)	N(4)–Re(2)–Cl(2)	82.79(19)
N(3)–C(12)–C(13)	112.3(7)	N(6)–C(42)–C(43)	111.7(7)
C(16)–C(19)–Br(1)	110.0(6)	C(46)–C(49)–Br(2)	111.3(7)
O(1)–C(1)–Re(1)	176.6(9)	O(4)–C(31)–Re(2)	177.7(9)
O(2)–C(2)–Re(1)	179.1(8)	O(5)–C(32)–Re(2)	178.7(9)
O(3)–C(3)–Re(1)	179.3(8)	O(6)–C(33)–Re(2)	178.0(9)

**1** and **2** were soluble in most organic solvents, but compound **3** proved extremely insoluble in most organic solvent, and only slightly soluble in DMF and MeCN, making recrystallization and characterization more difficult.

Compounds **1–3** were satisfactorily characterized by elemental analyses, ESI–MS, IR and <sup>1</sup>H NMR spectroscopy, and by X-ray crystallography for **1** and **2**. The ESI–MS revealed that the molecular ion fragments [M], [M + H]<sup>+</sup> or [M + Cl]<sup>–</sup> as the principal peaks with high abundance. Compounds **1–3** showed C=O stretches in the frequency range 1886–2025 cm<sup>-1</sup>. The <sup>1</sup>H NMR spectra showed that in most cases the signals of the proton of the coordinated pyridine and pyrazole ring were shifted to lower field with respect to the signals of the free ligand due to metal ion complexation, which agreed with the corresponding findings in other pyrazolyl–pyridyl-based complexes.<sup>20–22</sup>

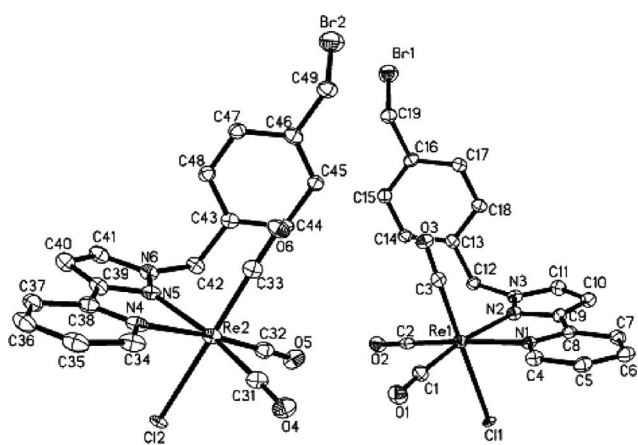
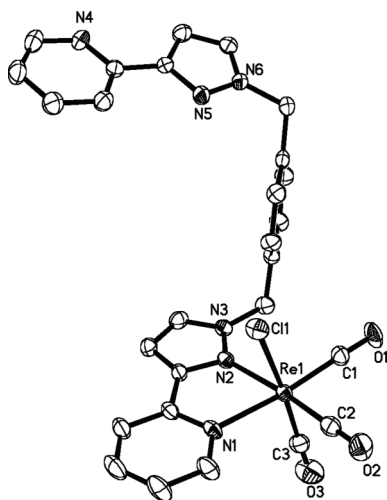
### Crystal structures

The solid state structures of **1** and **2** have been accurately determined by X-ray crystallography and ORTEP drawings of **1** and **2** are depicted in Fig. 1 and 2, respectively. Details of the data collection and refinement are given in Table 1. Selected bond lengths and angles for the molecules are listed in Table 2 and 3, respectively. Both complexes feature distorted octahedral coordination with three CO groups being *fac*-oriented around the Re(I) center. The relevant bonding lengths and angles around the Re(I) center are in the normal ranges as observed in similar [Re(N–N)(CO)<sub>5</sub>Cl] (N–N = diimine complexes).<sup>27</sup>

As shown in Fig. 1, the pyridine ring and the pyrazole ring are almost coplanar with a dihedral angle of 4.7°. The bromomethyl substituted phenyl ring plane is almost orthogonal to the pyrazolyl–pyridine ring plane with a dihedral angle of 85.8°. In

**Table 3** Selected bond distances (Å) and angles (°) for complex **2**

Re(1)–C(1)	1.868(4)	C(3)–Re(1)–N(2)	95.00(18)
Re(1)–C(2)	1.880(5)	C(1)–Re(1)–N(1)	173.95(15)
Re(1)–C(3)	1.891(5)	C(2)–Re(1)–N(1)	98.29(15)
Re(1)–N(2)	2.142(3)	C(3)–Re(1)–N(1)	93.59(16)
Re(1)–N(1)	2.145(3)	N(2)–Re(1)–N(1)	73.33(12)
Re(1)–Cl(1)	2.4073(12)	C(1)–Re(1)–Cl(1)	95.30(14)
C(3)–O(3)	1.056(6)	C(2)–Re(1)–Cl(1)	90.25(15)
C(1)–O(1)	1.122(5)	C(3)–Re(1)–Cl(1)	174.88(13)
C(2)–O(2)	1.124(5)	N(2)–Re(1)–Cl(1)	84.68(9)
C(1)–Re(1)–C(2)	86.76(18)	N(1)–Re(1)–Cl(1)	81.42(9)
C(1)–Re(1)–C(3))	89.77(19)	O(1)–C(1)–Re(1)	178.3(4)
C(2)–Re(1)–C(3)	89.4(2)	O(2)–C(2)–Re(1)	179.2(4)
C(1)–Re(1)–N(2)	101.38(15)	O(3)–C(3)–Re(1)	175.8(5)
C(2)–Re(1)–N(2)	170.75(14)	N(6)–C(26)–C(23)	112.1(3)

**Fig. 1** ORTEP drawing of **1** showing two enantiomers with atom labeling scheme showing 30% thermal ellipsoids.**Fig. 2** ORTEP drawing of **2** with atom labeling scheme showing 30% thermal ellipsoids.

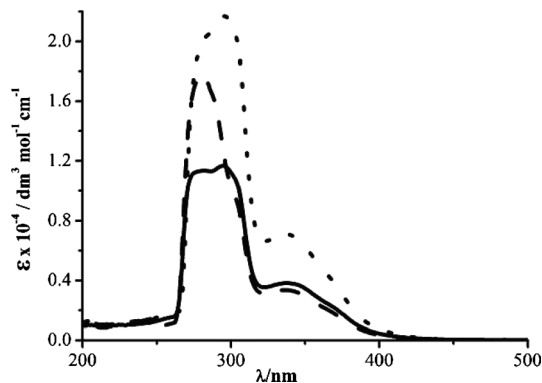
the complex **1** solid-state structure, there are several intermolecular hydrogen bonds and  $\pi \cdots \pi$  stacking interactions involving the phenyl ring and the pyrazolyl–pyridine ring, generating a unique supermolecular structure (Fig. S1†). The Cl atom serves as a hydrogen bond acceptor for three C atoms of the pyridine ring, the pyrazole ring and the bromomethyl substituted phenyl ring of three neighboring molecules (C–H $\cdots$ Cl in the range of 3.485–3.588 Å). A weak hydrogen bonding interaction is also

present between the oxygen atom of CO and the C atom of the methylene (C $\cdots$ O = 3.419 Å). In the case of complex **2** (Fig. 2), the ligand is slightly twisted, with the result that the angle between the coordinated and free pyrazolyl–pyridine rings is 22.2°. The coordinated pyrazolyl–pyridine ring plane is essentially orthogonal to the phenyl ring with a dihedral angle of 95.9°, while the dihedral angle of the free pyrazolyl–pyridine ring plane and the phenyl ring is 73.7°. Furthermore, the dihedral angle between the coordinated pyrazole ring and the pyridine ring is 1.5°, that is smaller than that of the free pyrazole ring and pyridine ring (5.9°), which is due to the complexation of the metal Re(I). Relatively weak intermolecular CH $\cdots$ Cl hydrogen bonds (C–H $\cdots$ Cl = 3.746 Å) and  $\pi \cdots \pi$  stacking interactions involving the free pyrazolyl–pyridine rings can be observed. A strong hydrogen bonding interaction is also present between the oxygen atom of CO and the C atom of the free pyrazole rings (C $\cdots$ O = 3.220 Å). This supermolecular association leads to formation of a two-dimensional sandwich (Fig. S2†). In addition, as shown in Fig. 1, two enantiomers are present in equal amounts in a well defined arrangement within the lattice of compound **1**, while for compound **2** only one specific enantiomer (Fig. 2) is selectively crystallized.

### Photophysical properties

The absorption and emission data of complexes **1–3** are summarized in Table 4. The electronic absorption spectra of **1–3** are characterized by an intense band at ca. 260–320 nm and a low-energy band at ca. 320–400 nm, which are typical of ligand-centered  $\pi \rightarrow \pi^*$  (pyrazolyl–pyridine) and MLCT [d(Re)  $\rightarrow$   $\pi^*$  (pyrazolyl–pyridine)] transitions,<sup>18,20–22,27,28</sup> respectively (Fig. 3). The electronic absorption spectra of **2** and **3** are similar, except that the absorption bands at high energy and low energy all have much higher intensity than those of the related complex **2**.

As listed in Table 4, compounds **1–3** exhibit bright yellow–green luminescence in the solid state and in solution at 298 K with excitation at  $\lambda_{\text{ex}} > 300$  nm. The solid state lifetime at 298 K is in the range of microseconds, revealing that the emission is most likely associated with a spin-forbidden triplet parentage.<sup>27,28</sup> All of these complexes exhibit almost the same emission maxima, centered at 506, 510 and 511 nm in the solid state. This indicates that the <sup>3</sup>MLCT excited states of the three complexes are almost the same and have the same energy levels, no matter what kind of

**Fig. 3** Electronic absorption spectra of **1** (solid), **2** (dash) in acetonitrile solution and **3** (dot) in DMF solution at room temperature.

**Table 4** Photophysical data for compounds **1–3**

Compound	Medium	$\lambda_{\text{abs}}/\text{nm}$ ( $\epsilon/\text{dm}^3 \text{ mol}^{-1} \text{ cm}^{-1}$ )	$\lambda_{\text{em}}/\text{nm}$ ( $\tau_{\text{em}}/\mu\text{s}$ ) <sup>a</sup> (298 K)	$\phi_{\text{em}}$ <sup>b</sup>
<b>1</b>	Solid	—	506 (1.25)	—
	MeCN	282 (11343), 295 (11665), 338 (3813)	538	0.040
<b>2</b>	Solid	—	510 (0.53)	—
	MeCN	281 (17904), 303 (9586), 336 (3346)	524	0.042
<b>3</b>	Solid	—	511 (0.64)	—
	DMF	285 (20472), 296 (21682), 337 (7075)	528	0.051

<sup>a</sup> The excitation wavelength in the lifetime measurement is 340 nm. <sup>b</sup> Relative to  $[\text{Ru}(\text{bpy})_3]^{2+}$  ( $\phi_{\text{em}} = 0.062$ ).<sup>28</sup>

ligand is present in the molecules. The average value of *ca.* 510 nm for the emission maxima is blue shifted by *ca.* 85 nm from that of the similar complex  $[\text{Re}(\text{bpy})(\text{CO})_3\text{Cl}]$ ,<sup>28</sup> which is due to the higher  $\pi^*$  orbital (LUMO) energy of pyrazolyl–pyridine ligand compared to that of the bpy ligand with the result of increasing the energy gap between HOMO and LUMO. The emission in MeCN at room temperature (Fig. 4), however, is red-shifted *ca.* 14–32 nm as compared to that in the solid state. This phenomenon is typical of phosphorescence from the  $[\text{d}(\text{Re}) \rightarrow \pi^*(\text{pyrazolyl-pyridine})]$  <sup>3</sup>MLCT excited state, which has been reported in many rhenium(i) diimine tricarbonyl complexes in the literature.<sup>18,27–28</sup> It is noteworthy that quantum efficiencies of luminescence of compounds **1–3** are found to lie between 0.040 and 0.051, as measured using  $[\text{Ru}(\text{bpy})_3]^{2+}$  ( $= 0.062$ ) as a relative standard, which are much higher than that of the  $[\text{Re}(\text{bpy})(\text{CO})_3\text{Cl}]$  complex ( $= 0.019$ ).<sup>18,28</sup>

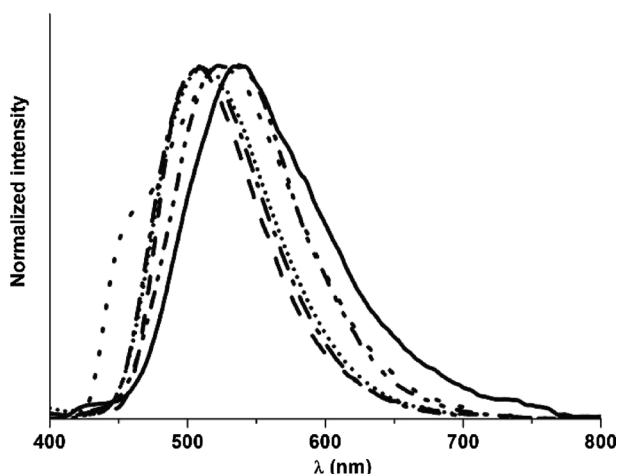


**Fig. 4** Emission spectra of **1** (solid), **2** (dot), **3** (dash dot dot) in acetonitrile solution and **1** (dash), **2** (dash dot) and **3** (short dot) in the solid states at room temperature.

### Electrochemistry and electrochemiluminescence (ECL)

The redox behaviors of homo- or binuclear complexes **1–3** ( $1 \times 10^{-3} \text{ mol L}^{-1}$ ) and ligands L1, L2 ( $1 \times 10^{-3} \text{ mol L}^{-1}$ ) were determined by cyclic voltammetry (CV) and differential pulse voltammetry (DPV) using  $\text{Bu}_4\text{NPF}_6$  ( $c = 0.1 \text{ mol L}^{-1}$ ) as the supporting electrolyte in deaerated acetonitrile solution. All electrochemical data for the three rhenium complexes and the free ligands are collected in Table 5. The free ligand L1 shows one irreversible reduction wave at  $-1.09 \text{ V}$ , while L2 exhibits two irreversible reduction waves at  $-1.06$  and  $-1.28 \text{ V}$ , respectively (as shown in Fig. S3†).

As shown the cyclic voltammogram in Fig. 5, complexes **1** and **3** display one irreversible oxidation wave ( $I_{\text{pa}} < I_{\text{pc}}$ ), while complex **2** shows one quasi-reversible oxidation wave ( $\Delta E = 70 \text{ mV}$ ,  $I_{\text{pa}} : I_{\text{pc}} \approx 1$ ). This oxidation has been assigned to the  $\text{Re(I)}/\text{Re(II)}$  redox reaction. The more positive oxidation potential for **1** ( $E_{1/2} = 1.43 \text{ V}$ ) compared with **2** ( $E_{1/2} = 1.41 \text{ V}$ ) is due to the better electron withdrawing ability of L1 than that of L2. The oxidation potentials of **1–3** are more positive than that obtained for the reference  $[\text{Re}(\text{bpy})(\text{CO})_3\text{Cl}]$  ( $E_{1/2} = +1.32 \text{ V}$ ),<sup>29</sup> which indicates that complexes **1–3** are more difficult to oxidize. In the cathodic region, one irreversible reduction wave is observed in the cyclic voltammograms of complexes **1–3** (as shown in Fig. S4†), which is assigned to the reduction of the pyrazolyl–pyridyl-based ligand ( $\text{L} \rightarrow \text{L}^-$ ). For complex **1** and **2**, the reduction wave is not equal in area to the oxidation wave, while no oxidation wave is found in the cathodic region of complex **3**. The irreversibility of the reduction wave follows the order **1** < **2** < **3**. In agreement with the electron withdrawing ability of the free ligands L1, L2, the reduction potential of **1** is less negative than that of **2**. The reduction potentials of the three present rhenium complexes are all more negative than that obtained in the reference  $[\text{Re}(\text{bpy})(\text{CO})_3\text{Cl}]$  ( $E_{1/2} = -1.35 \text{ V}$ ),<sup>29</sup> which is due to the higher  $\pi^*$  orbital (LUMO) energy of the pyrazolyl–pyridine ligand than that of the bpy ligand.

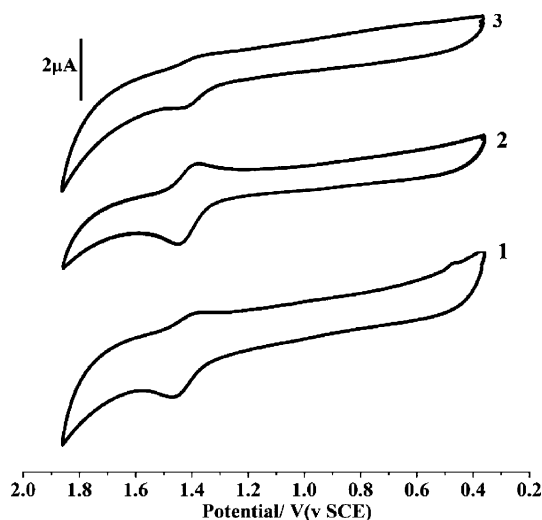


**Fig. 5** CVs of  $1 \text{ mmol L}^{-1}$  **1**, **2** and **3** in deaerated acetonitrile solution at scan rate of  $100 \text{ mV s}^{-1}$ .

Under the experimental conditions and over the range of scan rates from  $10$  to  $400 \text{ mV s}^{-1}$ , the dependence of the anodic peak current of the  $\text{Re(I)}/\text{Re(II)}$  redox pair of the complexes **1–3** was

**Table 5** Electrochemical data for complexes **1–3** and ligands L1, L2

Compound	$E_p$ (V) <sup>a</sup>			Reduction (V)		
	Oxidation (V)			Reduction (V)		
	$E_{pa}$	$E_{pc}$	$E_{1/2}$	$E_{pa}$	$E_{pc}$	$E_{1/2}$
L1				-1.09		
L2				-1.06, -1.28		
<b>1</b>	+1.39	+1.47	+1.43	-1.43	-1.38	1.40
<b>2</b>	+1.38	+1.45	+1.41	-1.45		
<b>3</b>	+1.36	+1.42	+1.39		-1.40	
[Re(bpy)(CO) <sub>3</sub> Cl]			1.32 <sup>b</sup>	-1.35 <sup>b</sup>		

<sup>a</sup> All potentials were determined at room temperature in deaerated MeCN solutions (0.1 M Bu<sub>4</sub>NPF<sub>6</sub>) vs. SCE at scan rate of 100 mv s<sup>-1</sup>. <sup>b</sup> From values reported in ref. 29 in deaerated MeCN solutions.

investigated to identify the type of current. With the increase of the scan rate, the oxidation and reduction peak currents of the complexes **1–3** are increased markedly, and the ratio of them ( $I_{pa} : I_{pc}$ ) is also increased. The peak currents and scan rate show good linear relationships, which indicates that the electrochemical process is controlled by absorption (as shown in Fig. S5†).<sup>7</sup>

ECL of a 50 μmol L<sup>-1</sup> solution of rhenium complexes **1–3**, containing 0.1 mol L<sup>-1</sup> Bu<sub>4</sub>NPF<sub>6</sub> was observed when the potential of the Pt working electrode was pulsed between the oxidation and reduction waves of the three rhenium complexes (~ +1.8 and -2.0 V). The ECL spectra are similar to the photoluminescence spectra, so the same <sup>3</sup>MLCT states are probably formed in both experiments.<sup>18</sup> It is noted that **3** displays the highest ECL intensity owing to the existence of two [Re(CO)<sub>3</sub>Cl] groups in the structure. No ECL emission was observed on scanning to potential less positive or negative than those needed to form the anionic and cationic species, respectively. The generation of luminescence upon pulsing the potential could be explained by analogy to the well-studied [Re(L)(CO)<sub>3</sub>Cl] (L = bpy, 1,10-phenanthroline (phen), or a methyl-substituted derivative) system.<sup>18,19</sup>

Coreactant system ECL also has been studied using 50 μM solution of the rhenium complexes at the Pt working electrode with tri-*n*-propylamine (TPrA) or 2-(dibutylamino)ethanol (DBAE) as the coreactant. As shown in Fig. 6–7, the ECL intensity peaks of three rhenium complexes **1–3** with TPrA as the coreactant appear at potentials of 1.61 V, 1.55 V and 1.60 V, respectively, whereas with DBAE as the coreactant (Fig. 7) at more negative potentials of 1.53 V, 1.43 V and 1.50 V, respectively, which may be attributed to the easier oxidation of DBAE than TPrA.<sup>31</sup> It is found that the ECL intensities of complexes **1–3** are all influenced by the concentration of TPrA and DBAE. As shown in Fig. 8, the ECL intensities of complexes **1–3** are increase noticeably with the increasing concentration of DBAE. With the same DBAE concentration, ECL intensity follows the order **1** > **2** > **3**. When TPrA is the coreactant, a maximum of the ECL intensities in all the complexes **1–3** can be observed along with the increasing concentration of TPrA. With the same TPrA concentration, ECL intensity follows the order **2** > **1** > **3**. When the concentrations of TPrA and DBAE are lower than about 60 mM, the ECL intensity of the complexes **1–3**-TPrA system is higher than that of the DBAE system. In most cases, the ECL quantum efficiencies of complexes **1–3** are comparable to that of the [Re(L)(CO)<sub>3</sub>Cl] (L = bpy or phen) system<sup>18</sup> (Table 6). It is noted that oxygen tended to substantially decrease the ECL intensities of the three

**Table 6** ECL quantum efficiencies of complexes **1–3**

Compounds	Annihilation <sup>a</sup>	1–3-coreactant system <sup>b</sup>	
	( $\phi_{ECL}$ )	( $\phi_{ECL,TPA}$ )	( $\phi_{ECL,DBAE}$ )
<b>1</b>	0.00176	0.0602	0.0212
<b>2</b>	0.00161	0.0693	0.0227
<b>3</b>	0.00852 <sup>c</sup>	0.0255	0.0131
[Re(bpy)(CO) <sub>3</sub> Cl] <sup>d</sup>	0.00029	0.52	—
[Re(phen)(CO) <sub>3</sub> Cl] <sup>d</sup>	0.00064	0.087	—

<sup>a</sup>  $\phi_{ECL}$  were calculated with respect to the ECL efficiency of Ru(bpy)<sub>3</sub><sup>2+</sup> of  $\phi_{ECL} = 0.0500$  in MeCN.<sup>30</sup> Reported values were averaged from at least five scans with a relative standard deviation of ~10% in MeCN solutions.

<sup>b</sup>  $\phi_{ECL}$  calculated with respect to  $\phi_{ECL} = 1.00$  for Ru(bpy)<sub>3</sub><sup>2+</sup>. ECL solutions contained 1 μM complex and 0.025 mol L<sup>-1</sup> TPA or DBAE. <sup>c</sup> In DMF solution. <sup>d</sup> From the reported values in ref. 18.

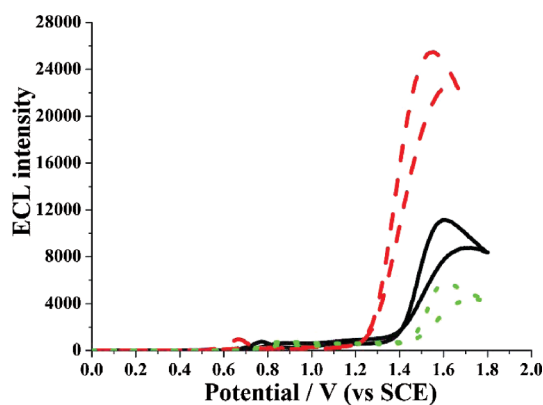


**Fig. 6** ECL intensity–potential curve of 50 μmol L<sup>-1</sup> **1** (solid), **2** (dash) and **3** (dot) in acetonitrile solution containing 35 mmol L<sup>-1</sup> TPrA.

rhenium complexes when the TPrA concentration is lower than 10 mM. Fig. 9 shows that the ECL intensity of **1** deaerated for 5 min is about six times higher than that in air-saturated solution, then when oxygen is added into the solution the ECL intensity is gradually decreased, which could enable it to be used as an oxygen sensor.

## Conclusions

Three rhenium carbonyl complexes **1–3** were prepared by reaction of the appropriate bidentate pyrazolyl–pyridyl-based ligand with [Re(CO)<sub>3</sub>Cl]. These complexes exhibit bright yellow–green

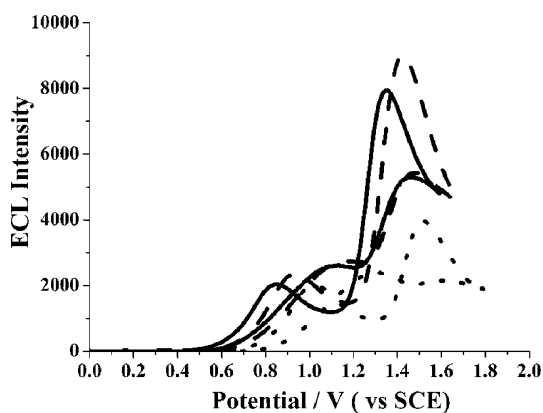


Fig. 7 ECL intensity-potential curve of 50  $\mu\text{mol L}^{-1}$  **1** (solid), **2** (dash) and **3** (dot) in acetonitrile solution containing 35  $\text{mmol L}^{-1}$  DBAE.

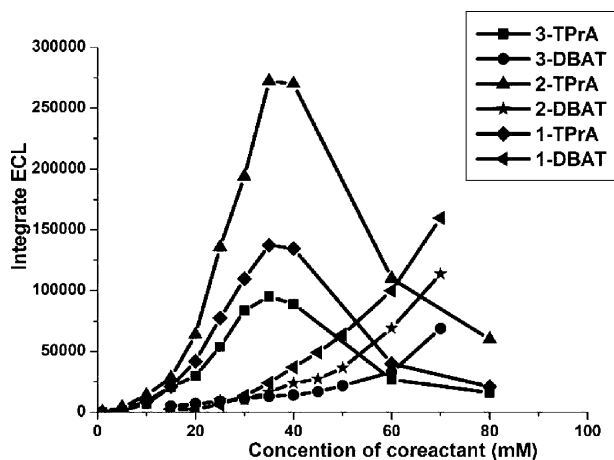


Fig. 8 ECL intensity of complexes **1–3** vs. the concentration of the TPrA and DBAE coreactant.

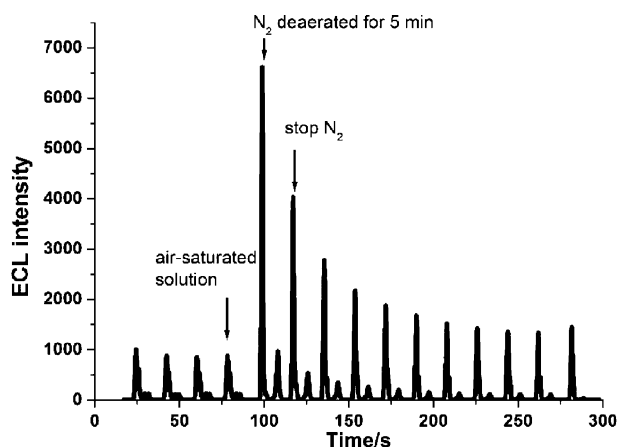


Fig. 9 ECL intensity of 100  $\mu\text{mol L}^{-1}$  complex **1** in air-saturated and nitrogen gas deaerated (for 5 min) acetonitrile solution containing 5  $\text{mmol L}^{-1}$  TPrA.

luminescence in the solid state and in solution at 298 K with lifetimes in the microsecond range, demonstrating spin-forbidden triplet  $^3\text{MLCT}$  excited states. Complexes **1** and **3** display a chemically irreversible metal-centered oxidation and an irreversible ligand-centered reduction, while complex **2** exhibits one quasi-reversible oxidation wave and also one irreversible ligand-centered

reduction wave. The ECL of the acetonitrile solutions of complexes **1–3** in the absence or presence of co-reactant tri-*n*-propylamine (TPrA) or 2-(dibutylamino)ethanol (DBAE) were observed by stepping the potential of a Pt disk working electrode. The ECL spectra were identical to the photoluminescence spectra, indicating that the chemical reactions following electrochemical oxidation or reduction form the same  $^3\text{MLCT}$  excited states. It was found that the concentration of TPrA and DBAE had a great effect on the ECL intensities of complexes **1–3**. The ECL quantum efficiencies of the complex **1–3**-TPrA systems are higher than that of the analogous systems with DBAE. In most cases, the ECL quantum efficiencies of complexes **1–3** are comparable to that of  $[\text{Re}(\text{L})(\text{CO})_2\text{Cl}]$  ( $\text{L} = \text{bpy}$  or  $\text{phen}$ ) system. It is noted that oxygen tends to substantially decrease the ECL intensities of the three rhenium complexes when the TPrA concentration is lower than 10 mM, which could enable them to be used as oxygen sensors.

## Acknowledgements

This study was financially supported by the National Nature Sciences foundation of China (20735002, 20801013, 20801014), the Innovation Foundation for Young Technological Talents of Fujian Province (2007F3050), and the project-sponsored by SRF for ROCS, SEM (LXKQ0830) and Fuzhou University (XRC-0723).

## Notes and references

- L. R. Faulker, and A. J. Bard, *Electroanalytical Chemistry*, Marcel Dekker, New York, 1977, vol. 10, p. 1; L. R. Faulker, and A. J. Bard, *Electrogenerated Chemiluminescence in Electrochemical Methods*, John Wiley and Sons, New York, 1980, p. 621; R. Y. Lai, E. F. Fabrizio, L. Lu, S. A. Jenekhe and A. J. Bard, *J. Am. Chem. Soc.*, 2001, **123**, 9112; I. Prieto, J. Teetsov, M. A. Fox, D. A. Vanden Bout and A. J. Bard, *J. Phys. Chem. A*, 2001, **105**, 520.
- M. M. Richter, *Chem. Rev.*, 2004, **104**, 3003.
- W. J. Miao, *Chem. Rev.*, 2008, **108**, 2506.
- M. Oyama and S. Okazaki, *Anal. Chem.*, 1998, **70**, 5079.
- L. Z. Hu and G. B. Xu, *Chem. Soc. Rev.*, 2010, **39**, 3275.
- D. M. Hercules, *Science*, 1964, **145**, 808; R. E. Visco and E. A. Chandross, *J. Am. Chem. Soc.*, 1964, **86**, 5350.
- Electrogenerated Chemiluminescence*, ed. A. J. Bard, Dekker, New York, 2004; A. J. Bard and L. R. Faulkner, *Electrochemical Methods: Fundamentals and Applications*, John Wiley and Sons, New York, 2nd edn, 2000, ch. 6.
- V. Balzani and A. Juris, *Coord. Chem. Rev.*, 2001, **211**, 97.
- A. Juris, V. Balzani, F. Barigelletti, S. Campagna, P. Belser and A. Von Zelewsky, *Coord. Chem. Rev.*, 1988, **84**, 85.
- N. E. Tokel and A. J. Bard, *J. Am. Chem. Soc.*, 1972, **94**, 2862.
- M. Zhou, G. P. Robertson and J. Roovers, *Inorg. Chem.*, 2005, **44**, 8317.
- S. Stagni, A. Palazzi, S. Zacchini, B. Ballarin, C. Bruno, M. Marccaccio, F. Paolucci, M. Monari, M. Carano and A. J. Bard, *Inorg. Chem.*, 2006, **45**, 695.
- H. Wei, J. Y. Yin and E. K. Wang, *Anal. Chem.*, 2008, **80**, 5635; X. B. Yin, S. J. Dong and E. K. Wang, *TrAC, Trends Anal. Chem.*, 2004, **23**, 432; Y. Du, H. Wei, J. Z. Kang, J. L. Yan, X. B. Yin, X. R. Yang and E. K. Wang, *Anal. Chem.*, 2005, **77**, 7993; H. Wei, Y. Du, J. Z. Kang and E. K. Wang, *Electrochem. Commun.*, 2007, **9**, 1474; X. P. Sun, Y. Du, S. J. Dong and E. K. Wang, *Anal. Chem.*, 2005, **77**, 8166.
- L. Dennany, R. J. Forster and J. F. Rusling, *J. Am. Chem. Soc.*, 2003, **125**, 5213.
- J. G. Li, Q. Y. Yan, Y. L. Gao and H. X. Ju, *Anal. Chem.*, 2006, **78**, 2694.
- W. J. Miao and A. J. Bard, *Anal. Chem.*, 2003, **75**, 5825; W. J. Miao and A. J. Bard, *Anal. Chem.*, 2004, **76**, 5379.
- D. Bruce and M. M. Richter, *Anal. Chem.*, 2002, **74**, 3157; A. Heller, *Faraday Discuss.*, 2000, **116**, 1; L. Dennany, R. J. Forster, B.

- White, M. Smyth and J. F. Rusling, *J. Am. Chem. Soc.*, 2004, **126**, 8835.
- 18 M. M. Richter, J. D. Debad, D. R. Striplin, G. A. Crosby and A. J. Bard, *Anal. Chem.*, 1996, **68**, 4370.
- 19 J. C. Luong, L. Nadjo and M. S. Wrighton, *J. Am. Chem. Soc.*, 1978, **100**, 5790.
- 20 Q. H. Wei, S. P. Argent, H. Adams and M. D. Ward, *New J. Chem.*, 2008, **32**, 73.
- 21 S. P. Argent, H. Adams, T. Riis-Johannessen, J. C. Jeffery, L. P. Harding, W. Clegg, R. W. Harrington and M. D. Ward, *Dalton Trans.*, 2006, 4996.
- 22 M. A. Halcrow, *Coord. Chem. Rev.*, 2005, **249**, 2880.
- 23 A. J. Amoroso, A. M. C. Thompson, J. C. Jeffery, P. L. Jones, J. A. McCleverty and M. D. Ward, *J. Chem. Soc., Chem. Commun.*, 1994, 2751.
- 24 S. P. Argent, H. Adams, L. P. Harding, T. Riis-Johannessen, J. C. Jeffery and M. D. Ward, *New J. Chem.*, 2005, **29**, 904; C. M. Hartshorn and P. J. Steel, *Inorg. Chem. Commun.*, 2000, **3**, 476.
- 25 G. M. Sheldrick, *SHELXL-97, Program for refinement of crystal structures*, University of Göttingen, Germany, 1997.
- 26 X. P. Wu, F. X. Huang, J. P. Duan and G. N. Chen, *Talanta*, 2005, **65**, 1279.
- 27 V. W. W. Yam, K. Z. Wang, C. R. Wang, Y. Yang and K. K. Cheung, *Organometallics*, 1998, **17**, 2440; V. W. W. Yam, V. C. Y. Lau and K. K. Cheung, *Organometallics*, 1995, **14**, 2749; E. R. Civitello, P. S. Dragovich, T. B. Karpishin, S. G. Novick, G. Bierach, J. F. O'Connell and T. D. Westmoreland, *Inorg. Chem.*, 1993, **32**, 237; Y. B. Dong, L. Q. Yang, K. K. Cheung and A. Mayr, *J. Organomet. Chem.*, 2000, **598**, 55; S. Das and B. K. Panda, *Polyhedron*, 2006, **25**, 2289.
- 28 J. V. Caspar and T. J. Meyer, *J. Phys. Chem.*, 1983, **87**, 952; J. V. Caspar and T. J. Meyer, *J. Am. Chem. Soc.*, 1983, **105**, 5583; J. Van Houten and R. J. Watts, *J. Am. Chem. Soc.*, 1976, **98**, 4853; L. A. Worl, R. Duesing, P. Y. Chen, L. D. Ciana and T. J. Meyer, *J. Chem. Soc., Dalton Trans.*, 1991, 849.
- 29 J. K. Hino, L. D. Della Ciana, W. J. Dressick and B. P. Sullivan, *Inorg. Chem.*, 1992, **31**, 1072.
- 30 H. S. White and A. J. Bard, *J. Am. Chem. Soc.*, 1982, **104**, 6891; I. Rubinstein and A. J. Bard, *J. Am. Chem. Soc.*, 1981, **103**, 512.
- 31 X. Q. Liu, L. H. Shi, W. X. Niu, H. J. Li and G. B. Xu, *Angew. Chem. Int. Ed.*, 2007, **46**, 421.